

Microstructures and mechanical properties of double hot-extruded AZ80+xSr wrought alloys

GUAN Shao-kang(关绍康), ZHU Shi-jie(朱世杰), WANG Li-guo(王利国),
YANG Qing(杨 卿), CAO Wen-bo(曹文博)

School of Materials Science and Engineering, Zhengzhou University, Zhengzhou 450002, China

Received 15 July 2007; accepted 10 September 2007

Abstract: The effects of Sr addition on microstructures and tensile properties of the as-cast and hot-extruded AZ80 alloys were studied by OM, SEM, EDS, XRD, DSC and Instron tester. The results show that the microstructures of as-cast alloys consist of α -Mg and β -Mg₁₇Al₁₂ phase. Sr gathers on the boundaries, and dissolves into β -Mg₁₇Al₁₂ phase or forms Mg₁₇Sr₂ phase. The grains of as-cast alloys are refined and discontinuous net-shaped structure is formed. The compound phases on the boundaries become thicker with increasing Sr content. The ultimate tensile stress(UTS) and elongation are improved compared with the corresponding Sr-free alloy. After preliminary hot-extruding, the UTS is up to 308–320 MPa and elongation reaches 8.0%–13.5%. After double hot-extrusion, the dynamic recrystallization completes totally, and the UTS is up to 310–355 MPa, but the elongation does not change apparently. The alloy with 0.02%Sr (mass fraction) obtains the best comprehensive performance with the UTS of 355 MPa and elongation of 13.2%. The SEM morphology of fracture surface shows that the alloys with Sr present good ductility after double hot-extrusion.

Key words: AZ80 magnesium alloy; Sr; double hot-extrusion; ultimate tensile strength; elongation

1 Introduction

Magnesium alloys are the lightest structural metallic materials with excellent properties such as high specific strength, superior damping characteristics, good moldability and electromagnetic shielding performance so they are paid great attention intensively as “the green project materials having development potential and best future in the 21st century”[1–4]. Because magnesium has HCP crystal structure with little slip system, plastic deformation is hard at room temperature[5]. At the same time, magnesium alloy castings exist many defects, such as unsound microstructure, low material utilization and reliability. Consequently its application is still limited to a narrow field. For conventional magnesium alloys, the strength and the elongation are not so high[6–7], which limits its application for structural use. Hot-forging, hot-extruding and hot-rolling are the efficiency ways to improve the formability of the magnesium alloys. Magnesium alloys produced by these methods can extend application range due to higher strength, better

plasticity and various mechanical properties. Therefore, ameliorating the process and improving the mechanical properties of wrought magnesium alloys are of great scientific significance[8]. Mg-Al-Zn alloys are the most widely used wrought alloys at present because of their abundant raw materials and low price. AZ80 alloy has attractive combination properties such as high strength, good plasticity and toughness. Sr has effect on refining grains and can improve the microstructures and properties[9]. In this work, the effects of Sr on microstructure and mechanical properties of both as-cast and hot-extruded AZ80 alloy were studied.

2 Experimental

Chemical compositions of the alloys are listed in Table 1. The raw materials are pure magnesium billets, pure zinc billets, pure aluminum billets, Al-Mn master alloy and Al-Sr master alloy. The actual absorption ratio of element may be considered when calculating the required amount of the raw materials. The alloys are melted in mild carbon steel stove under the cover of 5[#]

flux. When the stove was heated to approximate 500 °C, the covering agent is homogeneously laid at the bottom and magnesium billets were added and melted through heating to 720 °C. After billets were melted, pure zinc and pure aluminum were added. After their melting completely, the temperature was heated to 760–780 °C, and Al-Mn and Al-Sr master alloys were added. During the melting process, the liquid was stirred per 15 min to assure the homogeneity. At last the alloy was kept for 1 h at 740 °C. Semicontinuous casting was carried out at 700 °C under the protection of mixed gas of 1% SF₆ and 99% CO₂ (volume fraction).

The ingots were homogenized at 410 °C for 10–15 h, then were heated at (395±5) °C for 2 h, and hot-extruded twice at this temperature. The extrusion ratios are $\lambda_1=3.6$ and $\lambda_2=15$, respectively. The alloy samples were etched by carbazotic acid and ethanoic acid. The microstructures of both as-cast and hot-extruded alloys were observed with an optical microscope (OM,

Olympus H2-UMA). The phase identification was performed by an X-ray diffractometer(XRD, Philips-PW1700) using monochromatic Cu K α radiation. The morphology and energy spectrum were analyzed by using a scanning electron microscope(SEM, Philips-quanta-2000) equipped with an energy-dispersive X-ray spectrometer(EDS). The solution and eutectic temperatures of secondary phases of the alloys were measured with differential scanning calorimeter(DSC). Both as-cast and hot-extruded bars were machined into standard tensile specimens to measure their tensile properties (ultimate tensile strength and elongation) by an Instron 5585 material tester.

3 Results and discussion

3.1 Microstructures of as-cast alloys

Fig.1 shows the microstructures of as-cast alloys. The microstructures mainly consist of α -Mg and β -

Table 1 Chemical compositions of alloys (mass fraction, %)

Sample No.	Nominal composition					Actual composition				
	Al	Zn	Mn	Sr	Mg	Al	Zn	Mn	Sr	Mg
1-AZ80	8.5	0.5	0.12	0	Bal.	8.53	0.47	0.08	0	Bal.
2-AZ80+0.02%Sr	8.5	0.5	0.12	0.02	Bal.	8.63	0.5	0.08	0.018	Bal.
3-AZ80+0.16%Sr	8.5	0.5	0.12	0.16	Bal.	8.23	0.48	0.10	0.14	Bal.
4-AZ80+0.30%Sr	8.5	0.5	0.12	0.30	Bal.	8.33	0.44	0.091	0.30	Bal.

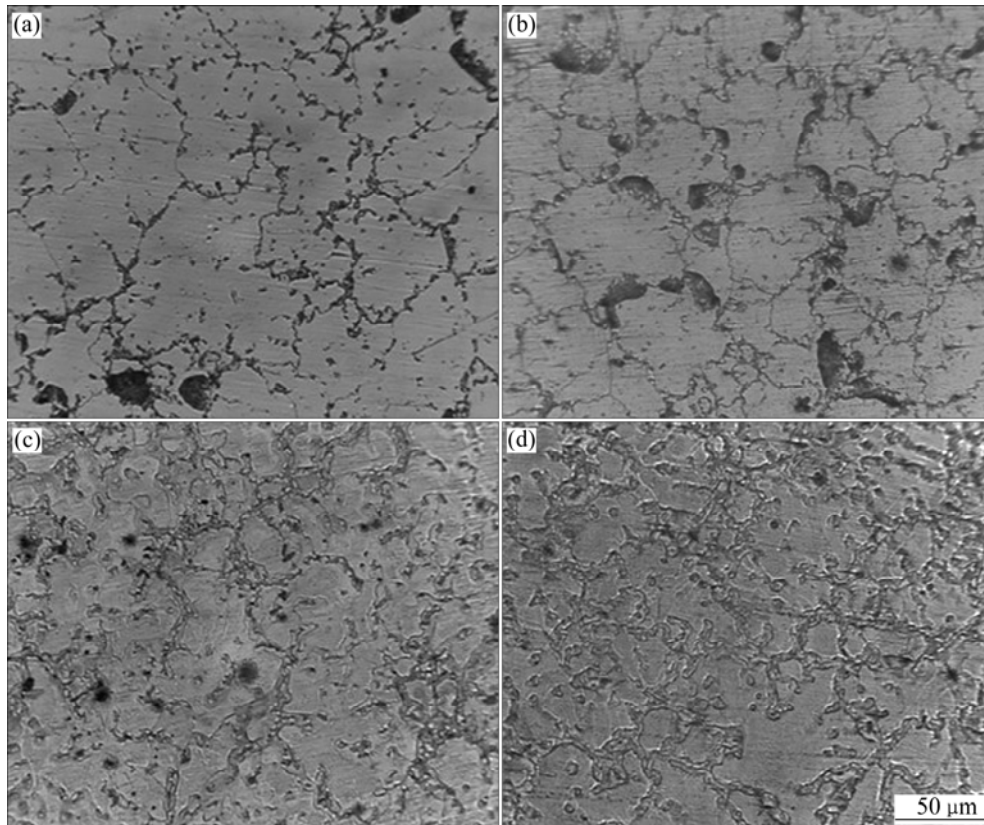


Fig.1 Optical micrographs of as-cast alloys: (a) Alloy 1; (b) Alloy 2; (c) Alloy 3; (d) Alloy 4

Mg₁₇Al₁₂ phase. β-Mg₁₇Al₁₂ phase gathers mainly on the boundaries and some dissolve into α-Mg crystalline. The grains of alloys with Sr addition are apparently smaller compared with Sr-free alloy. With increasing Sr content, the grain size becomes small apparently and phases on the boundaries become thicker. Discontinuous thick net-work structure can even be seen in alloys 3 and 4. Alloy 4 is not refined apparently compared with alloy 3, but the net-work structure of alloy 4 is thicker. All these illustrate that Sr can refine the alloys and change the state and distribution of β-phase. Sr is surface active element and has lower correlative solubility of 0.11% (mass fraction) in the α-Mg matrix. During the

solidification, Sr is pushed to the front of the solid/liquid interface. The congregated Sr on the interface of α-phase can bring ingredient over-cooling, effectively hindering the crystal growth and finally refining the grains. At the same time, Sr can improve the density and decrease shrinkage microporosity.

From SEM image of alloy 1 (Fig.2), sheet structure can be observed and according to EDS results, the grey part in Fig.2 can be confirmed to be Mg₁₇Al₁₂ phase, while the black part is α-Mg matrix.

The XRD patterns of the as-cast alloys are shown in Fig.3. For each alloy, the dominated phases are α-Mg and β-Mg₁₇Al₁₂. Zn dissolves into α-Mg and β-Mg₁₇Al₁₂

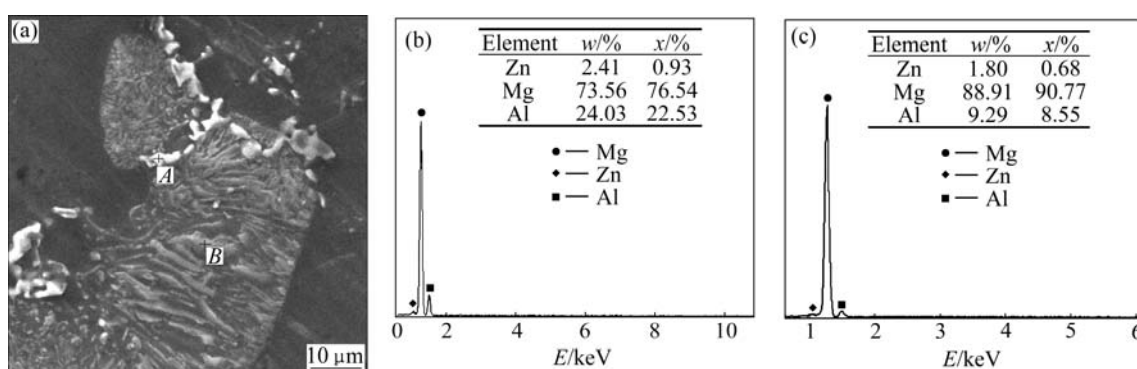


Fig.2 SEM image (a) and EDS patterns of A zone (b) and B zone (c) in Fig.2(a) of alloy 1

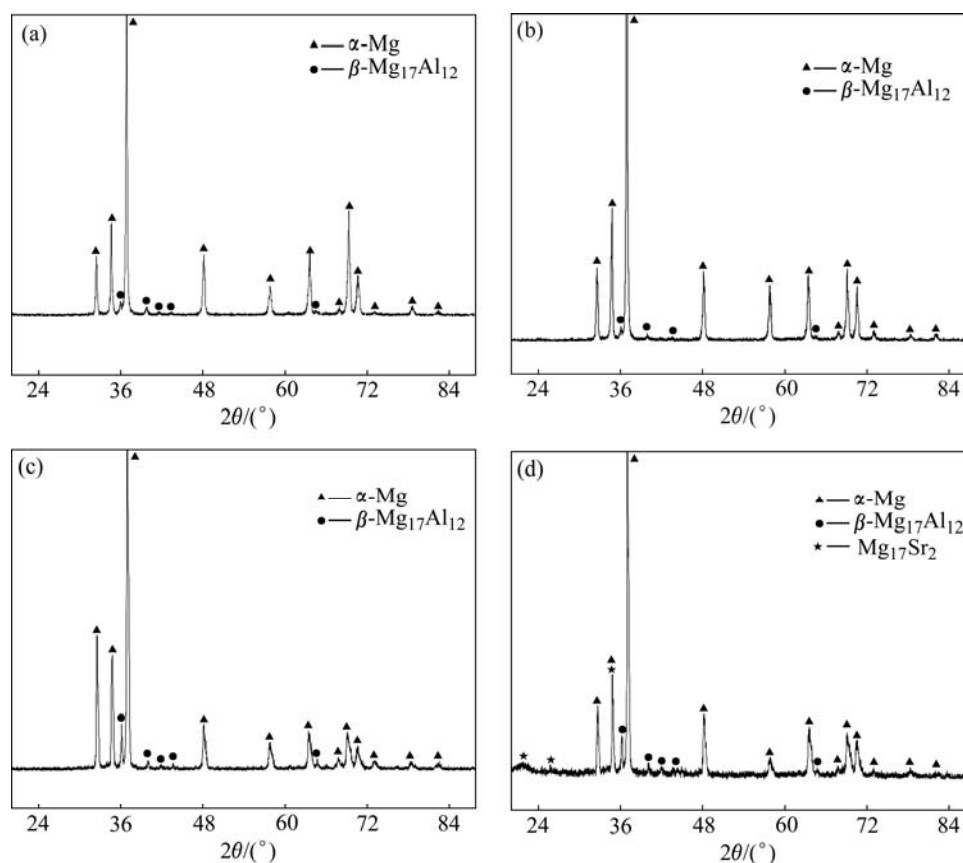


Fig.3 XRD patterns of as-cast alloys: (a) Alloy 1; (b) Alloy 2; (c) Alloy 3; (d) Alloy 4

phase[10–11]. No new phase is expected to form in alloys 2 and 3. Sr also dissolves into α -Mg matrix or β -Mg₁₇Al₁₂ compound phase for lower Sr content alloys. But the high-temperature stable Mg₁₇Sr₂ phase is found in alloy 4 because of higher Sr content. Because Mn can form Mg-Fe-Mn phase with Fe and then can be eliminated as sillage, Mn eliminates the harmful effect of Fe on magnesium alloys.

In order to determine the distribution of Sr, EDS spectrum and morphology analysis of as-cast and homogenized alloy 4 were carried out, as shown in Figs.4 and 5, respectively. Sr elements mainly gather in the net-work compounds on the boundaries. Mg₁₇Sr₂ phase is mixed with β -Mg₁₇Al₁₂ and cannot be observed from α -Mg matrix. So, Sr elements exist in the alloys as the following two states: some dissolve into β -Mg₁₇Al₁₂ phase and change the distribution of β -Mg₁₇Al₁₂ phase when Sr content is 0.02% and 0.16%; others form Mg₁₇Sr₂ phase on the boundaries when Sr content is up to 0.30%. Mg₁₇Sr₂ phase is high-temperature stable phase on the boundaries, and after the homogenization at 410 °C for 10 h it still cannot dissolve into the matrix. But β -Mg₁₇Al₁₂ phase is soft with relatively lower melting temperature and cannot pin the boundaries effectively. After homogenization, it dissolves into the matrix[12]. In Fig.5, the white zone is the mixture of Mg₁₇Sr₂ phase and

β -Mg₁₇Al₁₂ phase undissolved into the matrix.

3.2 DSC analysis of alloys

Fig.6 shows the DSC traces of the as-cast alloys at the heating rate of 20 °C/s. The temperature of the endothermic peaks in the DSC traces is listed in Table 2. Alloys 1, 2 and 3 have two endothermic peaks, at about 435 °C and 456 °C. From Mg-Al phase diagram[12] and the results of XRD analysis, the endothermic peak at about 435 °C corresponds to the eutectic reaction $L \rightarrow \alpha\text{-Mg} + \beta\text{-Mg}_{17}\text{Al}_{12}$, and the peak at about 456 °C corresponds to the melting of β -Mg₁₇Al₁₂ phase. There are three endothermic peaks on the DSC curves of alloy 4. They are at about 435, 570 and 650 °C. From Mg-Sr phase diagram, Mg-Al-Sr phase diagram[13] and the results of XRD analysis, the endothermic peak at about 435 °C corresponds to the eutectic reaction $L \rightarrow \alpha\text{-Mg} + \beta\text{-Mg}_{17}\text{Al}_{12}$, the peak at about 570 °C corresponds to the eutectic reaction $L \rightarrow \alpha\text{-Mg} + \text{Mg}_{17}\text{Sr}_2$, and the peak at about 605 °C corresponds to the melting of Mg₁₇Sr₂ phase. From the above DSC analysis, the highest eutectic temperature of the alloy 4 is about 570 °C, which is much higher than the eutectic temperature of Mg-Al binary alloy (435 °C). It can be inferred that the addition of Sr can greatly increase the eutectic temperature compared with that of Mg-Al binary alloy or form high-temperature stable Mg₁₇Sr₂ phase to hinder the

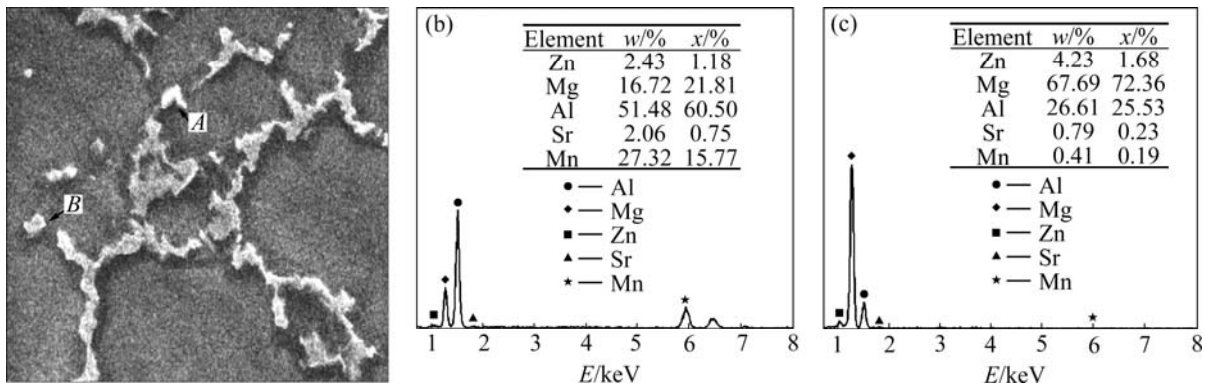


Fig.4 SEM image (a) and EDS patterns of A zone (b) and B zone (c) of as-cast alloy 4

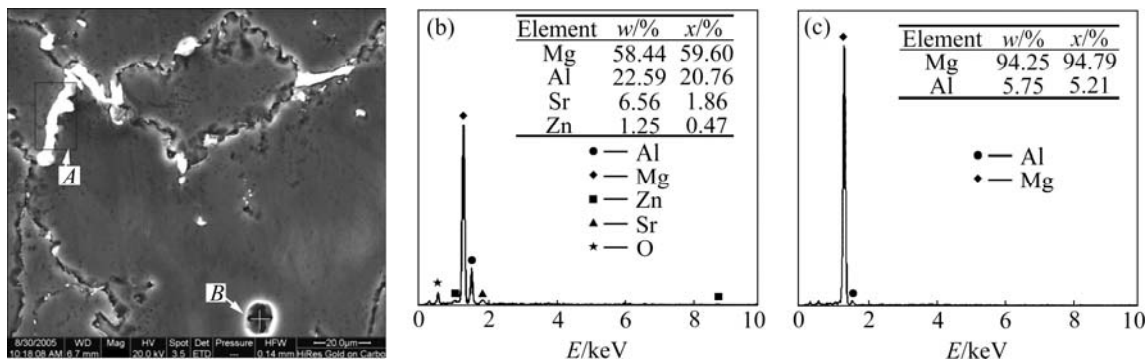


Fig.5 SEM image (a) and EDS patterns of A zone (b) and B zone (c) of homogenized alloy 4

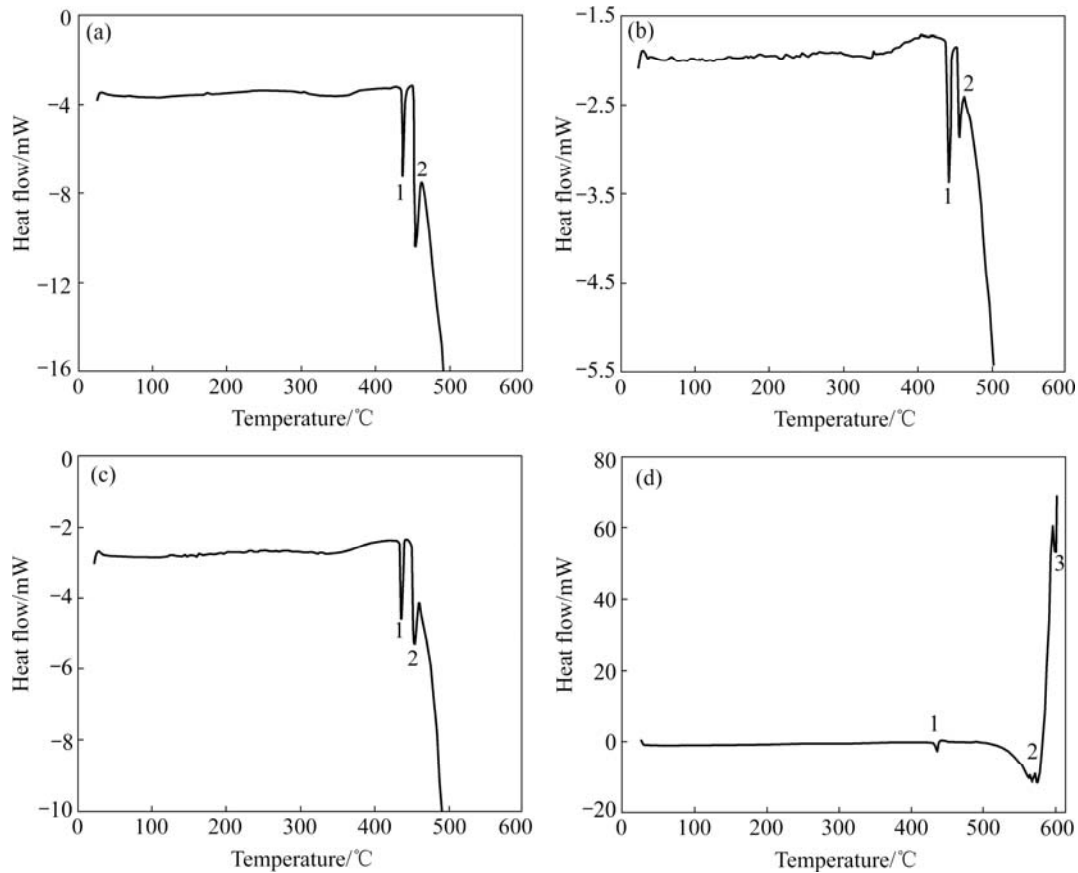


Fig.6 DSC traces of alloys at heating rate of 20 °C/min: (a) Alloy 1; (b) Alloy 2; (c) Alloy 3; (d) Alloy 4

Table 2 Transforming temperature of alloys on DSC traces

Alloy No.	Endothermic peak	Thermal signals/°C	Transforming temperature/°C	Reaction or phase boundary
1	1	437.41	435-447	$L \rightarrow \alpha\text{-Mg} + \beta\text{-Mg}_{17}\text{Al}_{12}$
	2	454.01	450-465	$L/L + \beta\text{-Mg}_{17}\text{Al}_{12}$
2	1	439.92	437-449	$L \rightarrow \alpha\text{-Mg} + \beta\text{-Mg}_{17}\text{Al}_{12}$
	2	452.85	450-463	$L/L + \beta\text{-Mg}_{17}\text{Al}_{12}$
3	1	436.66	433-445	$L \rightarrow \alpha\text{-Mg} + \beta\text{-Mg}_{17}\text{Al}_{12}$
	2	453.20	450-462	$L/L + \beta\text{-Mg}_{17}\text{Al}_{12}$
4	1	435.95	432-442	$L \rightarrow \alpha\text{-Mg} + \beta\text{-Mg}_{17}\text{Al}_{12}$
	2	568.22	549-580	$L \rightarrow \alpha\text{-Mg} + \text{Mg}_{17}\text{Sr}_2$
	3	605.95	595-610	$L/L + \text{Mg}_{17}\text{Sr}_2$

boundary migration. As a result, the grains of the alloy are refined. The grains of the as-cast-alloy 2 and alloy 3 is smaller than that of alloy 1. As a surface active element, Sr dissolves into $\text{Mg}_{17}\text{Al}_{12}$ phase and forms an absorbing film at the growing interface to decrease the growth rate, allowing that the melting liquid of alloy has effective refiner of Mg-Al alloys.

3.3 Microstructure of hot-extruded alloys

Because the range of solid/liquid two-phase zone is very large in Mg-Al alloys and Mg has HCP structure, the diffusion rate of alloying elements is decreased in Mg matrix and nonequilibrium crystalline phase and

segregation may be formed easily during the solidification. Due to the existence of $\beta\text{-Mg}_{17}\text{Al}_{12}$ phase, the plasticity of the alloys is worsened. Therefore, homogenizing treatment should be done before extrusion so that compound phase could dissolve into the matrix.

The $\beta\text{-Mg}_{17}\text{Al}_{12}$ phases in alloys 1, 2 and 3 nearly dissolve into the $\alpha\text{-Mg}$ matrix, while $\text{Mg}_{17}\text{Sr}_2$ phase in alloy 4 still exists on the boundaries with remained $\beta\text{-Mg}_{17}\text{Al}_{12}$, as shown in Fig.5.

The XRD results reveal that the phase constitution of the alloys show no change after extrusion and double-extrusion. Fig.7 shows the microstructures of the hot-extruded alloys. From Fig.7, the dynamic recrystalli-

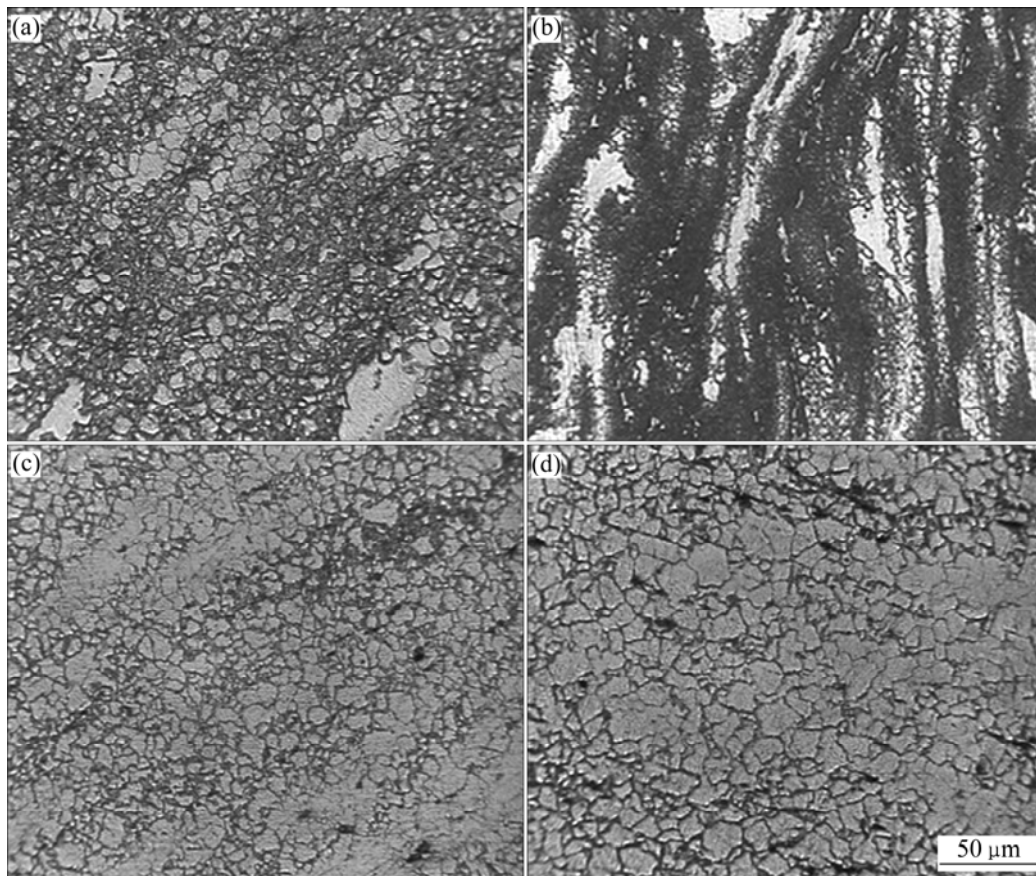


Fig.7 Optical micrographs (longitudinal direction) of preliminary hot-extruded alloys: (a) Sample 1; (b) Sample 2; (c) Sample 3; (d) Sample 4

zation(DRX) happens obviously in four alloys. Extruded orientation in alloy 1 is seen visibly, and large number of equiaxial grains exist along the extruded parallel lines. Parallel lines may be the recurrence of deformed fiber-texture in DRX structure. In the parallel lines, there are a large number of fine equal-axial grains. The microstructure of alloy 1 is composed of the mixture of originally undeformed grains and DRX grains. Extruded parallel lines and recrystallized equal-axial grains are the basic feature of deformed structures. But the DRX has almost happened completely and the extruded orientation can hardly be seen in the alloys 2, 3 and 4 with Sr addition. The extruded lines can also be seen, however are not clear as those in alloy 1. The structure is fine equiaxial grains, which is in favor of improving plasticity and strength to accelerate plastic deformation deeply of the alloys. The DRX is the assurance of higher elongation and successful deformation of magnesium alloys. The DRX happens in magnesium alloys during hot-extruding, because the fault energy of magnesium is low, especially its base-face fault energy (10 mJ/m^2). The large width of expanded dislocation make it difficult to escape from dislocation net, so it cannot be offset with opposite dislocation through coslipping and climbing to make the tendency of DRX increase. At the same time,

the grain size of as-cast Sr-contained alloys is very small and the deformation is very severe, which can provide effective conditions for DRX. The DRX can occur easily with additional extruding heat on original boundaries and new grain can nucleate and grow up adhering to the growing DRX[14].

After preliminary hot-extrusion, double hot-extrusion along the extruding direction and then air-cooling were carried out. Fig.8 shows the microstructures of four alloys after double hot-extrusion. The DRX can happen completely in four alloys during double hot-extrusion. The grain sizes are smaller compared with preliminary hot-extruding one. Fine equiaxial DRX grains can form and extruding orientation is not apparent. The alloys with Sr have larger and more homogeneous DRX grains. This is because high extrusion ratio can make alloys obtain higher deformation and higher density of dislocation to accelerate the speed of DRX and refine the grains. Alloy 1 has finer structure than that of primary extrusion. However, extrusion orientation can be seen and extruding orientation is not apparent. Alloys 3 and 4 have more coarse and homogeneous DRX structure than alloy 1 and alloy 2. Under the same extrusion condition, the

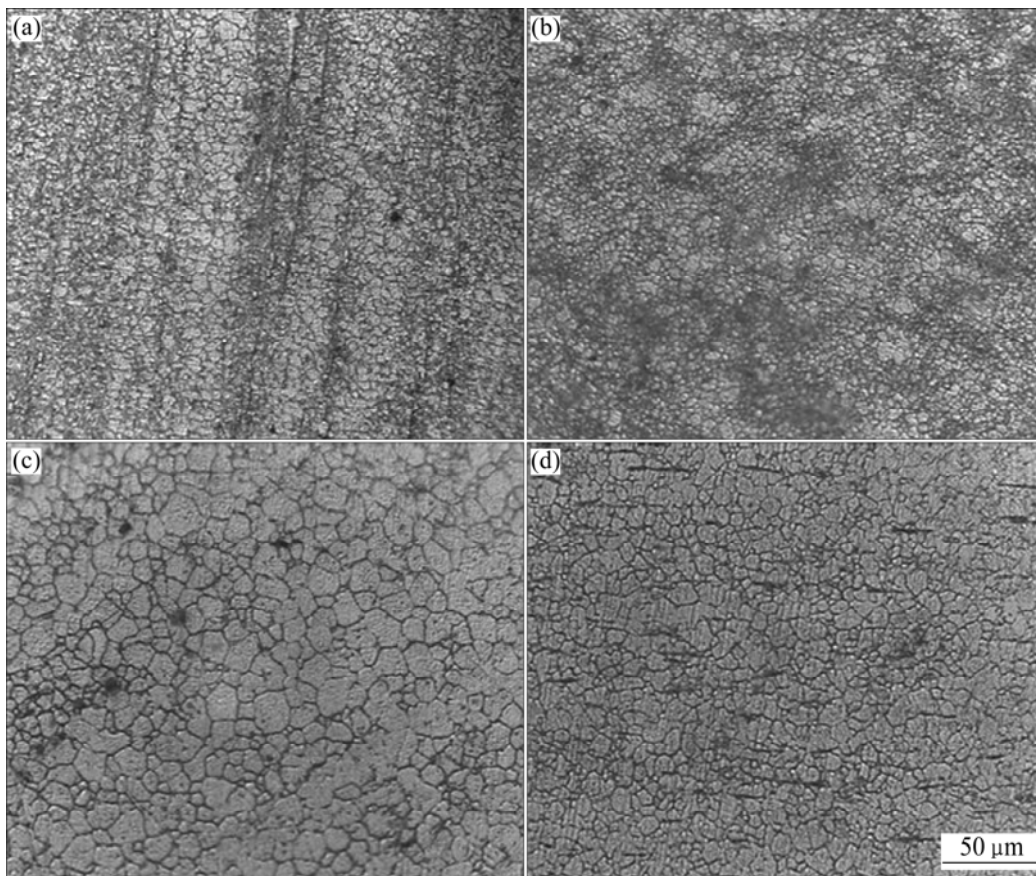


Fig.8 Optical micrographs (longitudinal direction) of double hot-extruded alloys: (a) Sample 1; (b) Sample 2; (c) Sample 3; (d) Sample 4

speed of dynamic recrystallization is so fast that new nucleus are swallowed before growing and then coarse structure can be formed. While alloys 3 and 4 have finer structure. The reason is that the high temperature stable $Mg_{17}Sr_2$ phase formed with 0.3%Sr inhibits the growth of DRX grains.

3.4 Tensile properties of alloys

The tensile properties of four alloys at different states are listed in Table 3. It can be seen that UTS and elongation of as-cast alloys 2, 3 and 4 with Sr are all improved compared with alloy 1. The UTS are increased by 20–25 MPa, and the elongation is improved by 40%–100%, respectively. The reason is that adding of Sr into magnesium alloys causes the grain sizes to apparently decrease, simultaneously affecting the precipitation and distribution of the second phases on the boundaries[15]. What's more, alloys 3 and 4 have more Sr content than alloy 2, and the net-structure second phases on the boundaries become relatively more and thicker, which can effectively hinder the moving of dislocations. Sliding deformation becomes worse and then the elongation of alloy 3 decreases. For alloy 4, $Mg_{17}Sr_2$ phase is formed, which makes net-work β phase

thicker and discontinuous on the boundaries. Consequently, the deformation becomes easier during tension and then the elongation is increased.

The properties of preliminary hot-extruded alloys are also listed in Table 3. Under the same state of preliminary hot-extrusion, the values of UTS of all alloys have no obvious difference, but the elongation is improved obviously with increasing Sr content. The elongation of alloys 3 and 4 is improved by above 60% compared with that of alloy 1. The reason may be that the structure of alloys 3 and 4 is more homogeneous and the DRX finishes wholly. But because of low extrusion ratio, the structure of alloy 1 is not homogeneous with mixed crystalline structure formed by DRX grains and bulk unbroken original structure during preliminary hot-extrusion. This shows that permanent stress still exists, which may decrease the plasticity and elongation of alloy. Compared with as-cast state, the UTS of preliminary hot-extruded state is increased by about 100 MPa, and the elongation is improved obviously by about 2–3 times. The strength is up to 308–320 MPa and the elongation reaches 8.0%–13.3%.

Plastic deformation can improve apparently the properties of alloys when the extrusion ratio is small.

The four alloys double hot-extruded directly after preliminary hot-extrusion only exhibit increased extrusion ratio under the same conditions. Table 3 shows the tensile properties after double hot-extrusion. It can be seen from Table 3 that the UTS and the elongation are increased appreciably after double hot-extrusion compared with preliminary hot-extruding state. The UTS of alloys 1 and 2 is improved by about 40 MPa to be over 350 MPa, but the elongation of alloy 1 is decreased a little. The elongation of alloy 2 is improved largely and increased by 2.5 times compared with alloy 1. The UTS and the elongation of alloys 3 and 4 show no apparent difference compared with alloy 2, but their UTS is lower than that of alloy 2. The reason is that larger grain sizes and less boundary cause lower resistance of hindering dislocation slipping. The DRX of alloys 3 and 4 grows

up quickly, the grains become coarse, but the grains of DRX of alloy 2 are more homogeneous and finer.

3.5 Morphologies of tensile fracture surface

Fig.9 shows the SEM images of the fractured surface of the double hot-extruded specimen after tensile test at room temperature. From Fig.9, the short and thin tearing ribs and a small quantity of deep dimples can be observed in the alloys containing Sr. This reveals that alloys present definite ductility. The fracture surfaces are composed of a small quantity of fleet dimples and a lot of cracked particles containing intermetallic compounds formed by Mg, Al and Sr. With increasing Sr content, the dimples become flatter and compounds become bigger and thicker. The SEM morphology of fracture surface shows that the alloys with Sr exhibit better ductility after

Table 3 Tensile properties of alloys

Sample No.	As-cast state		Preliminary hot-extruded state		Double hot-extruded state	
	σ_b /MPa	δ /%	σ_b /MPa	δ /%	σ_b /MPa	δ /%
1	186	2.5	312	8.0	351	5.8
2	210	5.1	320	9.6	355	13.2
3	205	3.6	310	12.5	315	13.9
4	210	4.5	308	13.3	310	13.1

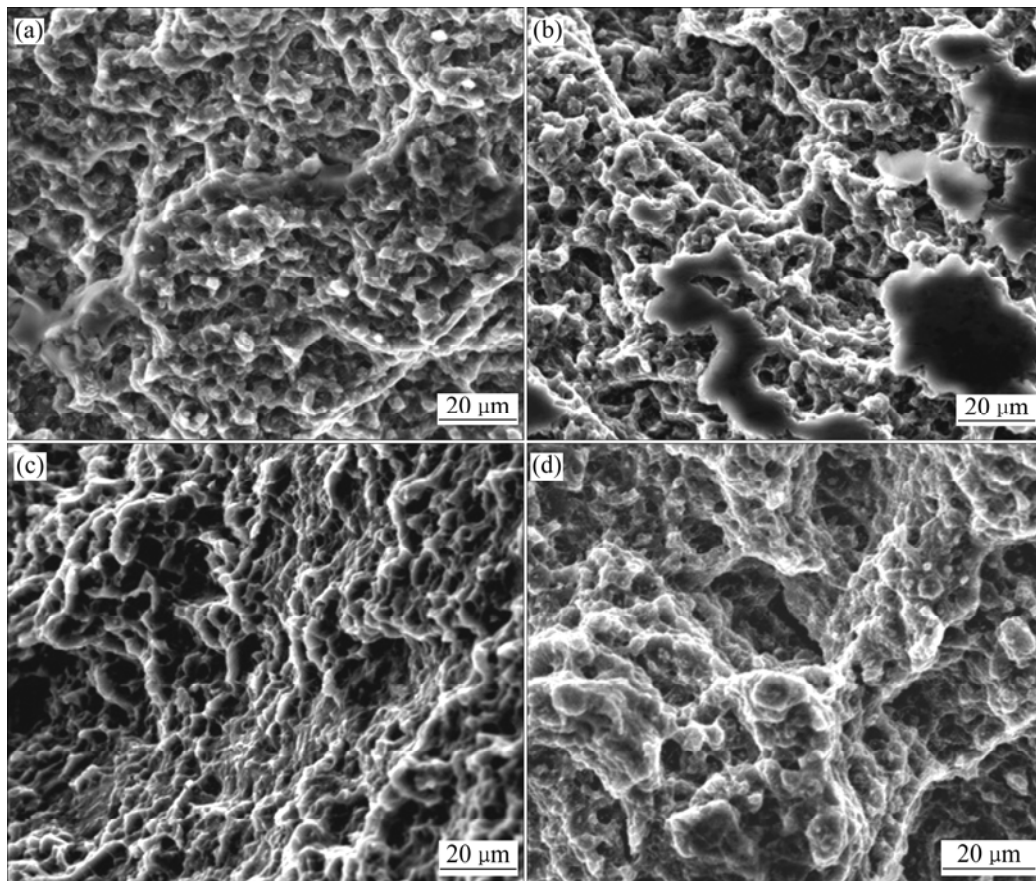


Fig.9 SEM fracture surface morphologies of double hot-extruded specimens at room temperature: (a) Sample 1; (b) Sample 2; (c) Sample 3; (d) Sample 4

double hot-extrusion than AZ80 alloy.

4 Conclusions

1) At as-cast state, microstructure of AZ80+xSr alloys consists of α -Mg and β -Mg₁₇Al₁₂ phase. Sr gathers mainly on the boundaries, Sr dissolves into β -Mg₁₇Al₁₂ phase or forms high-temperature Mg₁₇Sr₂ phase. The grains are refined and discontinuous thick net-shaped structure is formed. The UTS and elongation are increased by 20–25 MPa and above 40%, respectively.

2) After preliminary hot-extruding, the DRX of the alloys with Sr is completed relatively, but mixed structure of original grains and DRX grains is found obviously in AZ80 alloy. The UTS and elongation are improved obviously compared with as-cast alloys. The UTS is up to 308–320 MPa and the elongation reaches 8.0%–13.3%. Under the same state of preliminary hot-extrusion, the UTS of all alloys has no obvious difference, but elongation becomes higher with increasing Sr content.

3) After double hot-extrusion, DRX completes totally. the UTS and elongation are increased appreciably compared with preliminary hot-extrusion state. The UTS is up to 310–355 MPa, but the elongation does not change apparently. Alloy 2 with 0.02% Sr has the best comprehensive performance, that is, the UTS is 355 MPa and elongation is 13.2%. The SEM morphology of fracture surface shows that the alloys with Sr present good ductility after double hot-extrusion.

References

- [1] ALVES H, KOSTER U, AGHION E, ELIEZER D. Environmental behavior of magnesium and magnesium alloys [J]. *Material Technology*, 2001, 16(2): 110–126.
- [2] BAGHNI I M, WU Yin-shun, LI Jiu-qing, DU Cui-wei, ZHANG Wei. Mechanical properties and potential applications of magnesium alloys [J]. *Trans Nonferrous Met Soc China*, 2003, 13(6): 1253–1259.
- [3] ZENG Xiao-qin, WANG Qu-dong, LU Yi-zhe, DING Wen-jiang, ZHU Yan-ping. Recent development in applications of magnesium alloys [J]. *Foundry*, 1998, 47(11): 39–43.
- [4] ASM International. Magnesium and magnesium alloy [M]. OH: Metal Park, 1999.
- [5] LIU Zheng, ZHANG Kui, ZENG Xiao-qin. Theoretical foundation and application of light-quality magnesium-based alloys [M]. Beijing: Mechanical Industry Press, 2002: 16–37.
- [6] MORDIKE B L, EBERT T. Magnesium properties—applications—potential [J]. *Materials Science and Engineering A*, 2001, 302: 37–45.
- [7] ZHANG Ya, ZENG Xiao-qin, LIU Liu-fa, LU Chen, ZHOU Han-tao, LI Qiang, ZHU Yan-ping. Effects of yttrium on microstructure and mechanical properties of hot-extruded Mg-Zn-Y-Zr alloys [J]. *Materials Science and Engineering A*, 2004, 373: 320–327.
- [8] AGHION E, BRONFIN B, ELIEZER D. The role of the magnesium industry in protecting the environment [J]. *Journal of Materials Processing Technology*, 2001, 117: 381–385.
- [9] CHARTRAND P, PELTON A D. Critical evaluation and optimization of the thermodynamic properties and phase diagrams of the Al-Mg, Al-Sr, Mg-Sr and Al-Mg-Sr systems [J]. *Journal of Phase Equilibria*, 1994, 15(6): 591–605.
- [10] WANG Ling-yun, HUANG Guang-sheng, FAN Yong-ge, HUANG Guang-jie. Grain refinement of wrought AZ31 magnesium alloy [J]. *The Chinese Journal of Nonferrous Metals*, 2003, 13(3): 594–598. (in Chinese)
- [11] ZENG Xiao-qin, DING Wen-jiang, LU Chen. The microstructure and mechanical properties of Mg-Zn-Al alloys [J]. *Journal of Shanghai Jiaotong University*, 2005, 39(1): 46–51. (in Chinese)
- [12] ZHANG Jing, PAN Fu-sheng, GUO Zheng-xiao, DING Pei-dao, WANG Ling-yun. Development of alloy compounds in zirconium-free magnesium alloys [J]. *Heat Treatment*, 2003, 28(11): 6–11.
- [13] PARVEZA M A, MEDRAJ M, ESSADIQI E, MUNTASAR A, DÉNÈS G. Experimental study of the ternary magnesium-aluminium-strontium system [J]. *Journal of Alloys and Compounds*, 2005, 402: 170–185.
- [14] ION S E, HUMPHREYS F J, WHITE S H. Dynamic recrystallization and the development of microstructure during the high temperature deformation of magnesium [J]. *Acta Materialia*, 1982, 30(10): 1909–1919.
- [15] ZHU Shi-jie, CHEN Gui-lin, YANG Qing, GUAN Shao-kang. Microstructures of AZ80+xSr alloy and existing forms of Sr [J]. *Foundry Technology*, 2007, 28(1): 47–52.

(Edited by YANG Bing)